ACS APPLIED MATERIALS & INTERFACES

RESEARCH ARTICLE

www.acsami.org

Instantaneous Formation of Metal and Metal Oxide Nanoparticles on Carbon Nanotubes and Graphene via Solvent-Free Microwave Heating

Yi Lin,*[,†] David W. Baggett,[‡] Jae-Woo Kim,[†] Emilie J. Siochi,[‡] and John W. Connell*[,‡]

[†]National Institute of Aerospace, 100 Exploration Way, Hampton, Virginia 23666-6147, United States

[‡]Mail Stop 226, Advanced Materials and Processing Branch, NASA Langley Research Center, Hampton, Virginia 23681-2199, United States

Supporting Information

ABSTRACT: Microwave irradiation was shown to be an effective energy source for the rapid decomposition of organic metal salts (such as silver acetate) in a solid mixture with various carbon and noncarbon substrates under completely solvent-free conditions. The rapid and local Joule heating of microwave absorbing substrates (i.e., carbon-based) resulted in the instantaneous formation of metal and metal oxide nanoparticles on the substrate surfaces within seconds of microwave exposure. Other less absorbing substrates (such as hexagonal boron nitride) required longer exposure times for the salt decomposition to occur. Details of the effects of microwave reaction time, temperature, power, and other experimental parameters were investigated and discussed. The solvent-free microwave method was shown to be widely applicable to various organic metal salts with different substrates including single- and multiwalled carbon nanotubes, graphene, expanded graphite, hexagonal boron nitride and silica−alumina particles, forming substrate-supported metal (e.g., Ag, Au, Co, Ni, Pd, Pt) or metal oxide (e.g., Fe_3O_4, MnO, TiO_2) nanoparticles in high yields within short duration of microwave irradiation. The method was also successfully applied to large structural substrates such as nanotube yarns, further suggesting its application potential and versatility. To demonstrate one potential application, we successfully used both carbon nanotube powder and yarn samples decorated with Ag nanoparticles prepared via the above method to improve data acquisition in surface enhanced Raman spectroscopy.

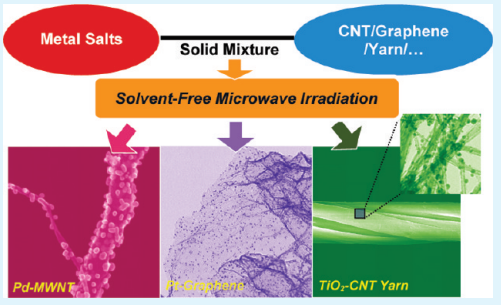

KEYWORDS: carbon nanotubes, graphene, microwave, nanohybrids, SERS, solvent-free

INTRODUCTION

Nanohybrids of metal or metal oxide nanoparticles supported on low-dimensional carbon nanomaterials have generated significant interest in various applications.[1−3] For example, Pd nanoparticle-decorated carbon nanotubes (CNTs)[4,5] and graphene[6,7] have both been used as effective heterogeneous catalysts for C−C bond forming reactions such as Suzuki and Heck reactions. The incorporation of various metal oxide nanostructures (e.g., titanium,[3,8−10] manganese,[11−15] tin,[16−18] and iron oxides[19−21]) on carbon nanomaterial surfaces rendered them useful as energy conversion or storage materials for applications in solar cells, supercapacitors, or Li-ion batteries. These unique applications took advantage of not only the specific physical and chemical properties of supported nanoparticles, but also the high surface area, light weight, high mechanical strength, and excellent electrical and thermal transport properties of the low-dimensional nanocarbon supports.

Since the first report in 1994,[22] the majority of solid-state preparations of metal nanoparticle-decorated CNTs have relied on the use of hydrogen gas to achieve the reduction of the corresponding metal salt. The use of solvents has been more popular because of the flexibility in the selection of benign chemical or electrochemical reduction processes as well as electroless strategies.[1,2] These solution methods for metal−carbon nanohybrids, however, are intrinsically challenging for large scale preparation due to, for instance, the multiple steps involved in these procedures and additional costs associated with the use and the removal of solvents and/or reducing reagents. We recently discovered a facile and highly scalable procedure in which metal or metal oxide nanoparticle-decorated CNTs could be produced by simply heating a solid physical mixture of CNTs and an organic metal salt (typically acetates and acetylacetonates) to a relatively low temperature (200−450 °C).[23−25] Without any additional reducing reagent or electrochemical process, thermal decomposition of the salts resulted in nanotube-supported zero-valence metal (e.g., Ag, Au, Co, Ni, Pd, and Pt) or metal oxide (e.g., Fe_3O_4 and ZnO) nanoparticles. It was shown that the size and distribution of the nanoparticles could be tuned by a variety of parameters such as mixing technique, metal salt loading, and

Received: February 18, 2011
Accepted: April 25, 2011
Published: April 25, 2011

substrate pretreatments. It was also demonstrated that the method was applicable to a wide variety of carbon and noncarbon substrates. Although the method is compatible with the use of solvents, the reactions were carried out under completely solvent-free conditions and are amenable to scaling to commercial quantities (~kilogram levels have been demonstrated[25]). In addition to conventional heating using a nitrogen oven, a few minutes of ball-milling was also found sufficient to provide mechanical energy required for partial decomposition of the metal salts in solid salt−nanotube mixtures to form nanotube-supported metal nanoparticles.[26]

Microwave irradiation has become a popular energy source of choice for organic synthesis in both fundamental research and the pharmaceutical industry.[27,28] Its applications in the synthesis of inorganic nanomaterials has also attracted significant attention.[29,30] An overwhelming majority of the nanomaterial syntheses using microwave energy have been conducted in liquids. The liquids, including typical solvents (i.e., water and polar organic solvents), ionic liquids, or the reactant itself, are generally responsible for microwave energy absorption to induce dielectric heating of the reaction mixture. The use of liquids provides many advantages for microwave heating over conventional heating for inorganic nanomaterials synthesis, such as high reaction rates, high yields, uniform heating, and often unique and excellent morphological control of the nanoscale products.[30] However, microwave synthesis of nanomaterials under solid-state conditions are still rare partially because most precursors such as organic salts have poor microwave absorptivities. There may also be a perception that the size and distribution of the nanoparticles cannot be controlled under solvent-free conditions.

Low-dimensional sp^2 carbon nanomaterials such as CNTs and graphene are excellent microwave absorbers due to their electrical conductivity.[31−38] Organic functionalization reactions of CNTs, which can take days using conventional heating,[39] could be achieved at similar yield within minutes under microwave irradiation in either dispersion[40−48] or solvent-free conditions.[49,50] In the latter circumstance, microwave-induced Joule heating of CNTs was likely responsible for the enhanced reaction rates of organic functional groups with the CNT surface.[31] Under the same principle, it is interesting to note that the "superheating" of CNTs from microwave irradiation was also utilized to cure CNT-based ceramic composites[51] or induce interfacial welding of CNT/polymer composites in the absence of solvents.[52] The application of microwave heating for graphene synthesis[53−56] and functionalization[57] are also under active development.

Previous efforts in the microwave preparation of metal or metal oxide nanoparticle-decorated CNTs[58−67] and graphene[20,68−72] were all conducted in the presence of a solvent, where in most cases the thermal reduction-deposition of metal ions was triggered by the dielectric heating of the solvent. In addition to using conventional heating[23−25] and mechanical energy[26] for the solvent-free preparation of metal or metal oxide nanoparticle-decorated CNTs, we now demonstrate that the direct solid-state Joule heating of CNTs or graphene with organic metal salts using microwave irradiation is a highly effective and versatile approach for the preparation of a wide variety of metal and metal oxide nanoparticle-decorated substrates. Although reactions using conventional heating may usually take at least an hour to complete, microwave heating of solid metal salt/substrate mixtures resulted in the near instantaneous formation of metal or metal oxide nanoparticles at excellent conversion yields.

EXPERIMENTAL SECTION

Materials. Silver(I) acetate (99%), cobalt(II) acetate (99.995%), iron(II) acetate (99.995%), nickel(II) acetate tetrahydrate (99.998%), palladium(II) acetate (99.9+%), platinum(II) acetylacetonate (99.99%), titanium(IV) oxyacetylacetonate (95%), and Rhodamine 6G (99%) were purchased from Aldrich. Gold(III) acetate and manganese(II) acetate were obtained from ESI Corp Inc. and Fisher Scientific Company, respectively. Multiwalled CNTs (MWCNTs; batch# UK115b) with a diameter range of ~20−150 nm were purchased from the University of Kentucky. Single-walled CNTs (SWCNTs; grade: AP-SWNT; batch#: AP-238) were obtained from Carbon Solutions, Inc. Graphene powder (Vor-X; grade: reduced 070; lot: BK-77x) was provided by Vorbeck Materials. Expanded graphite (EG) powder (grade: 3775; lot 3438) and hexagonal boron nitride (*h*-BN) powder (size −10P, Lot HZ010PA4.$06) were provided by Asbury Carbons and UK Abrasives, Inc., respectively. NASA/USGS lunar highlands dust simulant particles (NU-LHT-1D) (composed mainly of silica and alumina) were obtained from NASA Marshall Space Flight Center. Single ply CNT yarn (Lot #: Y3213−1(1)) was purchased from Nanocomp Technologies, Inc. All materials and chemicals were used as received.

Measurements. Scanning electron microscopy (SEM) and transmission electron microscopy (TEM) images were acquired using a Hitachi S-5200 field-emission SEM system under the secondary electron (SE) and transmitted electron (TE) modes, respectively. High-resolution TEM (HR-TEM) images and selected area electron diffraction (SAED) patterns were obtained on a JEOL 2100 field-emission transmission electron microscope. X-ray Diffraction (XRD) analyses were conducted on a Siemens D5000 X-ray diffractometer with Cu Kα as the radiation source (λ = 1.5418 Å). The obtained data were matched with the standard Powder Diffraction File (PDF) maintained by International Centre for Diffraction Data (ICDD). Raman spectroscopy measurements were performed using a Thermo-Nicolet-Almega Dispersive Raman Spectrometer with 532 nm excitation at 16% laser power (~3 mW) through a 100 μm pinhole. The acquisition of each spectrum consisted of 4 scans and totaled 16 s.

Microwave Reactions. In a typical model reaction for Ag nanoparticle-decorated MWCNTs, MWCNT powder (100 mg) was manually mixed with silver acetate powder in the desired ratio (typically 1 or 10 mol % Ag-to-C, corresponding to 8 or 47 wt %) using a mortar and pestle. The solid mixture was transferred to a standard 10 mL quartz vial for the microwave reactor (CEM Discover). The vial was then sealed with a septum, placed inside the reactor cavity, and further capped with a stainless steel pressurized top. The reaction was run at a set of desired reaction times (up to 60 min), temperatures (up to 300 °C), and power levels (up to 300 W). After reaction, the septum was removed from the quartz vial and the product was dried overnight either in air or with a moderate flow of nitrogen. Other experiments using different metal salt precursors or substrates were conducted in the same manner on a similar scale.

RESULTS AND DISCUSSION

Microwave reactions were carried out using the CEM Discover reactor by varying a set of parameters including hold time, temperature, and power level.[73] The Ag/MWCNT system was chosen as the primary model system for the microwave reactions because it has been thoroughly studied using conventional heating[23] and ball-milling[26] allowing for direct comparison with the microwave experiments discussed herein. In these reactions, the mixture of silver acetate and MWCNTs were heated using microwave irradiation, resulting in Ag nanoparticle-decorated MWCNTs. Although the thermal energy originated from a different source (i.e., microwave), the conversion of silver acetate salt to Ag metal occurred in a manner similar to that in the

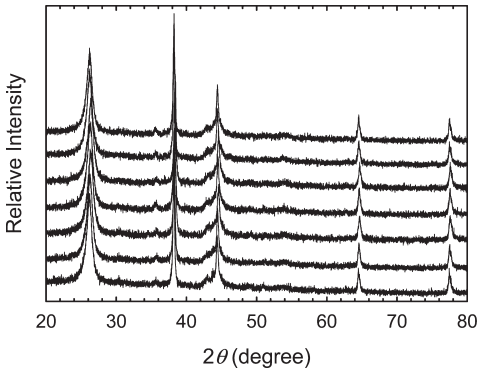

Figure 1. XRD patterns of various samples from modulated microwave irradiation (maximum power = 50 W, set temperature = 250 °C) of the same silver acetate/MWCNT starting material (1 mol % Ag-to-C content). The spectra from bottom to top correspond to hold times of 0, 1, 2, 5, 10, 30, and 60 min, respectively, after ramping to the set temperature.

well-known direct thermal decomposition of the salt.[23] During the conversion, MWCNTs acted as the supporting substrate for the templated formation of Ag nanoparticles from the silver acetate decomposition. It is important to point out that because byproducts such as acetic acid, CO_2, CO, and water were volatile, no additional product purification besides brief drying was required.

Effect of Hold Time. The "hold time" in the microwave experiments refers to the amount of time for which the reaction mixture was held at a set temperature after ramping to that temperature. In the previous study using conventional heating,[23] it was shown that the complete salt-to-metal conversion in silver acetate/MWCNT mixtures occurred at temperatures above 200 °C with 1−3 h holding in an oven with nitrogen atmosphere. Therefore, 250 °C was selected to be the set temperature for the first series of microwave experiments with varied hold times under "Standard Mode" operation, which provided modulated microwave heating. This means that the set microwave power level (50 W) was the maximum power the reactor could deliver during the entire course of heating. The actual power level in the microwave irradiation was automatically adjusted by the instrument program (typically <10 W after the first 10 s of ramping) in order to keep the temperature constant during the hold time. The programmed "run time" (i.e., ramp time) was set at 5 min, but the actual ramp times were much faster (~90 s) and the program automatically proceeded to "holding" once the infrared temperature sensor (at the bottom of the reactor cavity) detected the set temperature of 250 °C.

The same mixture of MWCNTs and silver acetate (1 mol % Ag-to-C content) was used as the starting material for each reaction, with modulated microwave heating to 250 °C at different hold times (1−60 min). Despite the difference in the hold times, the XRD patterns for the samples all exhibited signature patterns for MWCNTs at 26.2° (002) and metallic Ag (ICDD #04−0783) at 38.4° (111), 44.5° (200), 64.6° (220), and 77.5° (311), with the absence of silver acetate peaks (main peak at 29.2°, ICDD #14−0733) as shown in Figure 1. In addition, with normalized MWCNT (002) peaks, the Ag signals for these samples appeared with similar intensity, indicating complete salt-to-metal conversions for all samples with the hold time as short as 1 min (even for an experiment conducted without any set hold time, see the next section).

SEM images of these samples (Figure 2) showed abundant Ag nanoparticles distributed on the surface of MWCNTs. In general, the microscopic sample morphologies and the diameter/diameter distributions of Ag nanoparticles in all samples were comparable to one another. The diameter distributions of these Ag nanoparticles fell within the range of 20−100 nm and did not change significantly with different hold times except for a slight increase in the average diameter within the initial minutes. Compared to samples obtained by conventional heating using a nitrogen oven,[23] these microwave-formed Ag nanoparticles were of broader distribution and slightly larger in average size (~ 50 nm vs ~40 nm).

To assess the structural integrity of MWCNTs during the microwave induced reactions, Raman spectroscopy was conducted on the same Ag-MWCNT samples from different hold times of modulated microwave irradiation. Although the normalized spectra of these samples appeared rather similar (see Figure S1a in the Supporting Information), the attachment of Ag nanoparticles to MWCNTs resulted in the collective enhancement of the absolute intensity of the nanotube signals due to the well-known surface plasmon resonance of the Ag species, consistent with the reports in the literature.[74−77] The average enhancement factor of G-band (~1575 cm^{-1}) for the samples with 1 mol % Ag-to-C content was ~2.1 (see Figure S1b in the Supporting Information) and reached as high as 14 at 10 mol % (not shown). Compared to the spectrum of the pristine MWCNT sample, only a marginal increase was found for the intensity ratio of D-band (~1345 cm^{-1}) to G-band (I_D/I_G) even for the sample that was irradiated for as much as 60 min (see Figure S1c in the Supporting Information). It is unlikely that such change is due to the increase of MWCNT defect density from prolonged microwave irradiation because of its lack of consistent dependence on the hold time. It was shown previously that Ag nanoparticles preferably anchor on the nanotube defect sites when using conventional oven heating for silver acetate decomposition, resulting in higher enhancement factor for D-band intensity relative to G-band.[23] It is likely that the small overall I_D/I_G increase observed for the Ag-MWCNT samples from microwave irradiation was also from similar origin, namely the preferential growth of Ag nanoparticles at the defect sites of MWCNTs.

"No Hold" Runs. An important observation was that the same silver acetate/MWCNT mixture heated to 250 °C with modulated microwave heating (maximum power = 50 W) and no hold time also showed exactly the same XRD signatures (the bottom spectrum in Figure 1). The lack of silver acetate signals and presence of similar Ag peak intensities relative to those with much longer hold times strongly suggest that the salt-to-metal conversion was already complete during the temperature ramp, with further residence time at the set temperature having little to no effect on the conversion yield. To further investigate this phenomenon, experiments were carried out by only ramping the silver acetate/MWCNT mixtures to various temperatures below 250 °C with no temperature hold time.

Although the programmed temperature ramp time was 5 min, the actual ramp time for the solid mixtures was much more rapid, with shorter total duration at lower targeted temperatures.[78] This rapid heating is due to Joule heating associated with microwave absorbing substrates (MWCNTs in this case). For example, as shown in Figure 3, the time needed to heat a silver acetate/MWCNT mixture (10 mol % Ag-to-C) to 100 °C was only 6 s. As previously described,[23] the XRD intensity ratio of Ag (111) and

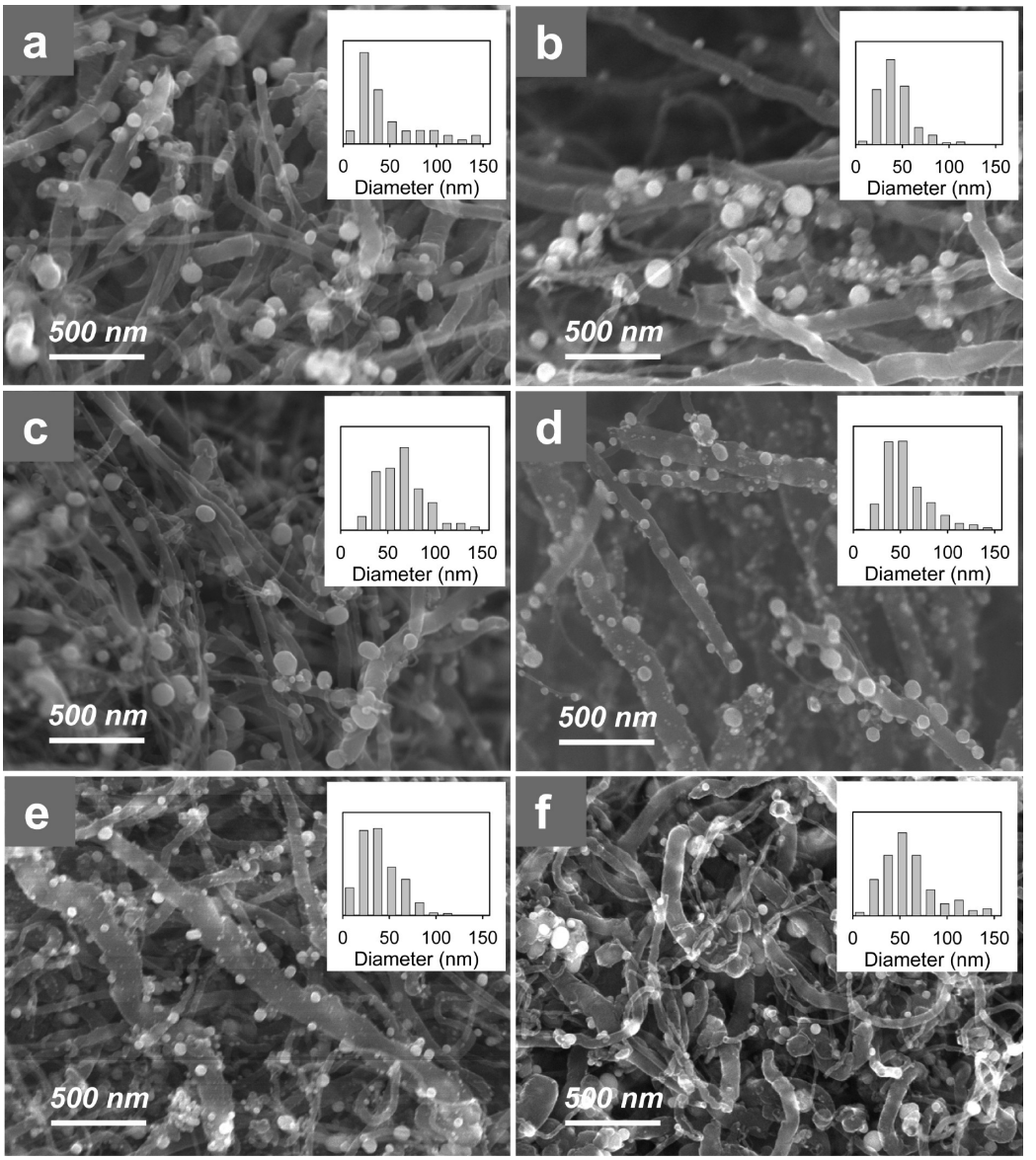

Figure 2. SEM images of various samples from modulated microwave irradiation (maximum power = 50 W, set temperature = 250 °C) of the same silver acetate/MWCNT starting material (1 mol % Ag-to-C content) for (a) 1, (b) 2, (c) 5, (d) 10, (e) 30, and (f) 60 min, respectively, after ramping to the set temperature.

MWCNT (002) peaks ($r = I_{Ag}/I_C$) could be used to estimate the salt-to-metal conversion yield by using a reference sample. In the current experiments, the samples heated to 250 °C with no hold time were used as the complete conversion references (no silver acetate peak seen in XRD, see Figure 1). As also shown in Figure 3, the salt-to-metal conversion was essentially complete at 150 °C with ~10 s of modulated microwave irradiation in spite of the Ag content in the sample increasing to 10 mol %. Even with only a "flash" of microwave energy of 1 s (set temperature of 35 °C), Ag nanoparticles were instantaneously formed with a significant salt-to-metal conversion of greater than 60%. This strongly indicates that the excellent microwave absorption characteristics of MWCNTs produced a much higher local temperature on their surfaces under microwave conditions than the temperature in the quartz vial measured by the infrared temperature sensor.

At relatively lower Ag contents (i.e., 1 mol % Ag-to-C), the diameters of Ag nanoparticles on MWCNTs obtained with no hold time and heated to different final temperatures fell into slightly smaller size ranges (~15 − 60 nm) than those synthesized with various hold times (Figure 4; also see Figure 1). When the Ag content was increased to 10 mol %, as shown in Figure 5, the sizes of most Ag nanoparticles became significantly larger (>90 nm) than those at 1 mol % Ag-to-C at the same reaction conditions (heating to 250 °C with no hold time). This same phenomenon was observed in the use of conventional heating.[23] Similarly, it is possible that this is also due to the presence of a limited number of active nanotube surface anchoring sites (such as defects). Thus, samples with a higher metal content quickly saturated the anchoring sites; consequently the remaining decomposed material continued depositing on the original seeds, resulting in nanoparticles of larger sizes.

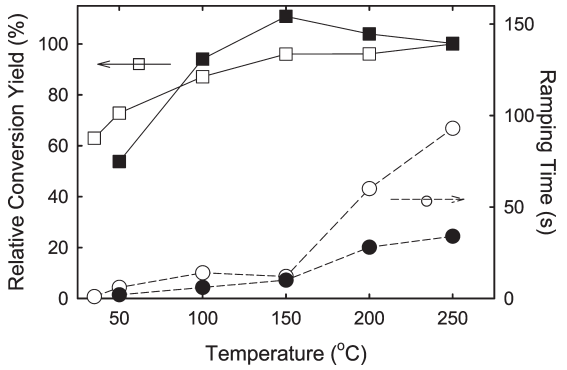

Figure 3. Relative conversion yields (squares) and the temperature ramp times (circles) of silver acetate/MWCNT mixtures at 1 mol % (open symbols) and 10 mol % Ag-to-C content (solid symbols) with modulated microwave heating (maximum power =50 W) to different set temperatures without further holding. The relative conversion yields were calculated by $(\text{yield}\%)_T = [(I_{Ag}/I_C)_T/(I_{Ag}/I_C)_{250\ °C}] \times 100\%$, where I_{Ag} and I_C are the intensities of Ag (111) and MWCNT (002) peaks, respectively, and T corresponds to the set temperature.

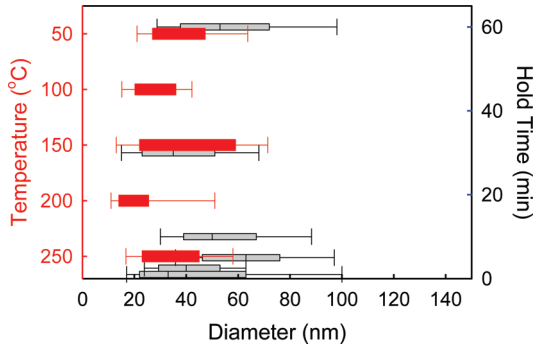

Figure 4. Ag nanoparticle diameter distributions (red symbols) for the same silver acetate/MWCNT starting material (1 mol % Ag-to-C content) after modulated microwave heating (maximum power = 50 W) to different set temperatures (red *y*-axis on the left) without further holding. Those from further holding for different times (black *y*-axis on the right) at 250 °C (gray symbols) were also shown for comparison.

It is worthwhile to note there were many smaller nanoparticles (<20 nm in diameter) present in the sample with 10 mol % Ag-to-C content shown in Figure 5b. Such phenomenon (also noted to a lesser degree in conventional heating) was consistently observed and much more pronounced in samples with higher metal content and irradiated with higher power (see next Section). This may suggest an incomplete thermodynamic process in which the kinetically formed smaller Ag nanoparticles were yet to be annealed into the larger ones due to the rate of microwave heating.

Effect of Microwave Power. The formation of Ag nanoparticles on MWCNTs was also studied by varying the microwave irradiation power under the "Power-Time Mode" with the reactor or continuous microwave heating. Except for this section, all other experiments in the present study used the "Standard Mode" or modulated microwave heating. Under the "Power-Time Mode", the microwave power was kept constant until the defined maximum temperature was reached. For traditional microwave reactions in solution, the maximum temperature can usually be set at a higher value in order to keep the reaction running at constant power feed. For the solid-state reactions in this report, however, the maximum temperature (maximum 300 °C for the reactor) was usually easily reached, and the continuous microwave irradiation was automatically terminated by the reactor safety shutdown protocol.

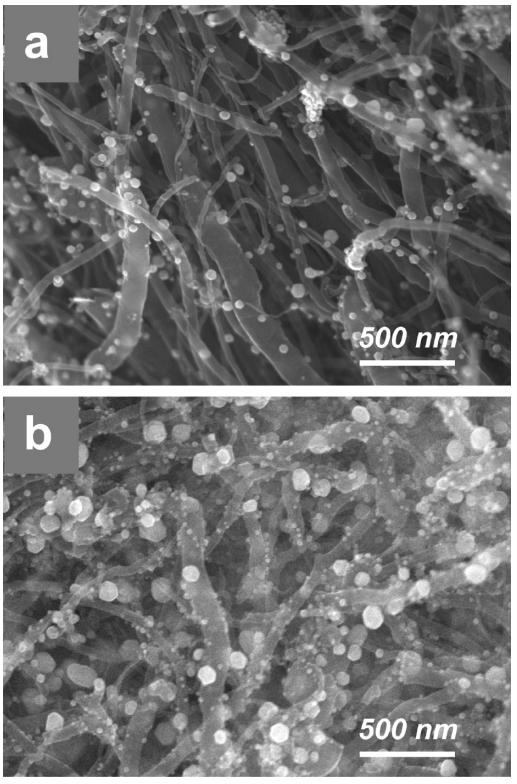

Figure 5. SEM images of samples from modulated microwave irradiation (maximum power = 50 W, set temperature = 250 °C) of silver acetate/MWCNT mixtures with Ag-to-C content of (a) 1 and (b) 10 mol %, respectively.

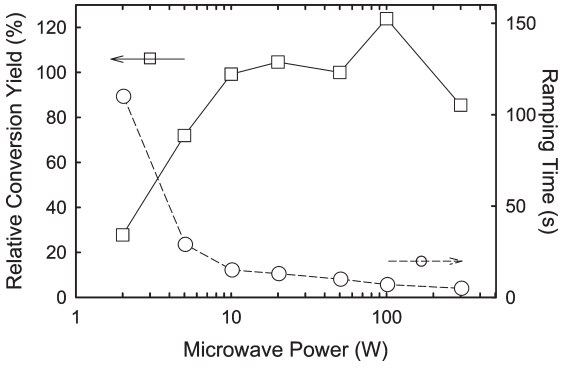

Figure 6. Relative conversion yields (□) and the temperature ramping times (○) of silver acetate/MWCNT mixtures with 10 mol % Ag-to-C content with continuous microwave heating (set temperature =150 °C) at different power levels. The relative conversion yields were calculated by $(\text{yield}\%)_P = [(I_{Ag}/I_C)_P/(I_{Ag}/I_C)_{50W}] \times 100\%$, where P corresponds to the set power.

As described in the section above, the set temperature of 150 °C was found to be sufficient for the complete salt-to-metal conversion in the silver acetate/MWCNT systems using "no hold" modulated microwave heating with 50 W maximum power. Therefore, 150 °C was chosen to be the maximum temperature

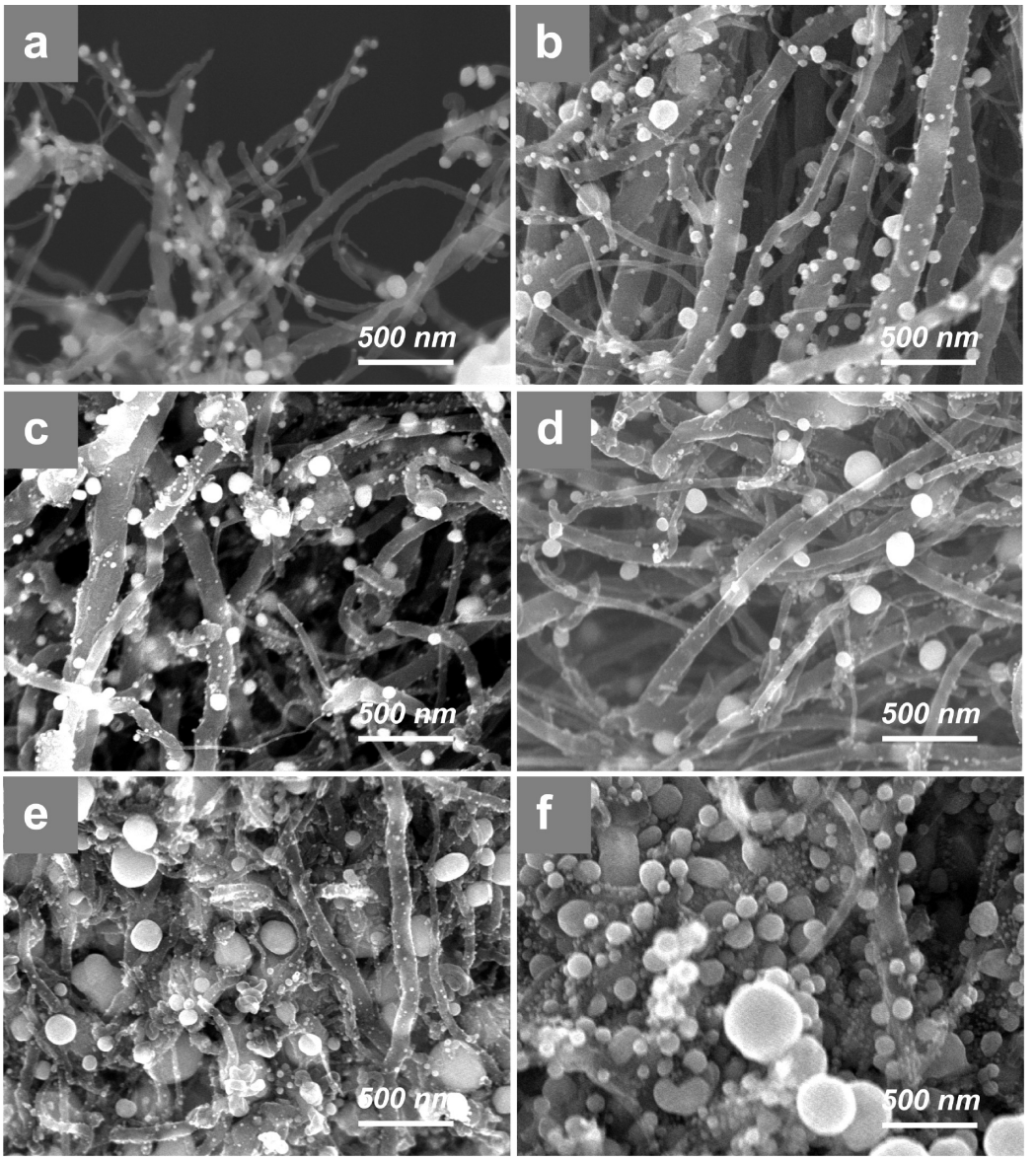

Figure 7. SEM images of samples from continuous microwave heating (set temperature = 150 °C) of silver acetate/MWCNT mixtures with 10 mol % Ag-to-C content. The irradiation power levels were at (a) 2, (b) 5, (c) 10, (d) 50, (e) 100, and (f) 300 W, respectively.

and the constant microwave power was varied in the range of 2−300 W under the "Power-Time Mode" to irradiate the silver acetate/MWCNT mixtures with 10 mol % Ag-to-C content. In all of these experiments, the reactor shut down automatically as soon as the maximum temperature was reached and there were no further temperature holds. For example, as shown in Figure 6, it took 110 s for the system to climb to 150 °C at 2 W with <30% salt-to-metal conversion (with the sample from 50 W used as the complete conversion reference). The conversion was complete when the microwave power was increased to 10 W with only ∼15 s of ramp time. It is interesting to note that the actual power level in the "no hold" modulated microwave heating to 150 °C (see previous section) was mostly at ∼10 W. Increasing microwave power resulted in decrease of ramp time despite similarly complete conversion. The continuous microwave irradiation seemed to have enhanced the local Joule heating at both MWCNTs and initially formed Ag nanoparticles to yield larger metal nanoparticles at higher irradiation power (Figure 7). However, because of the rapid rate of the heating, there was again a significant amount of much smaller nanoparticles (<10 nm), which might also be attributed to an incomplete thermodynamic process.

Decoration with Metal vs Metal Oxide Nanoparticles. Short microwave exposure could also decompose many other organic metal salts to form the corresponding metal or metal oxide nanoparticles on the surface of various substrates. For example, ∼30 s of "no-hold" runs with modulated microwave heating to 150 °C (maximum power = 50 W) was sufficient to decompose the majority of both palladium acetate and iron acetate (thermal decomposition thresholds at ∼170 and ∼230 °C, respectively) in their respective mixtures with MWCNTs at metal-to-C contents of ∼10 mol %. Under such conditions, the resultant nanohybrids consisted of MWCNTs with densely decorated metallic Pd (average diameter ∼25 nm) or Fe_3O_4 nanoparticles (average diameter ∼15 nm) as shown in images a and b in Figure 8. The XRD patterns showed the progressive increase as a function of set temperature of the signature peaks

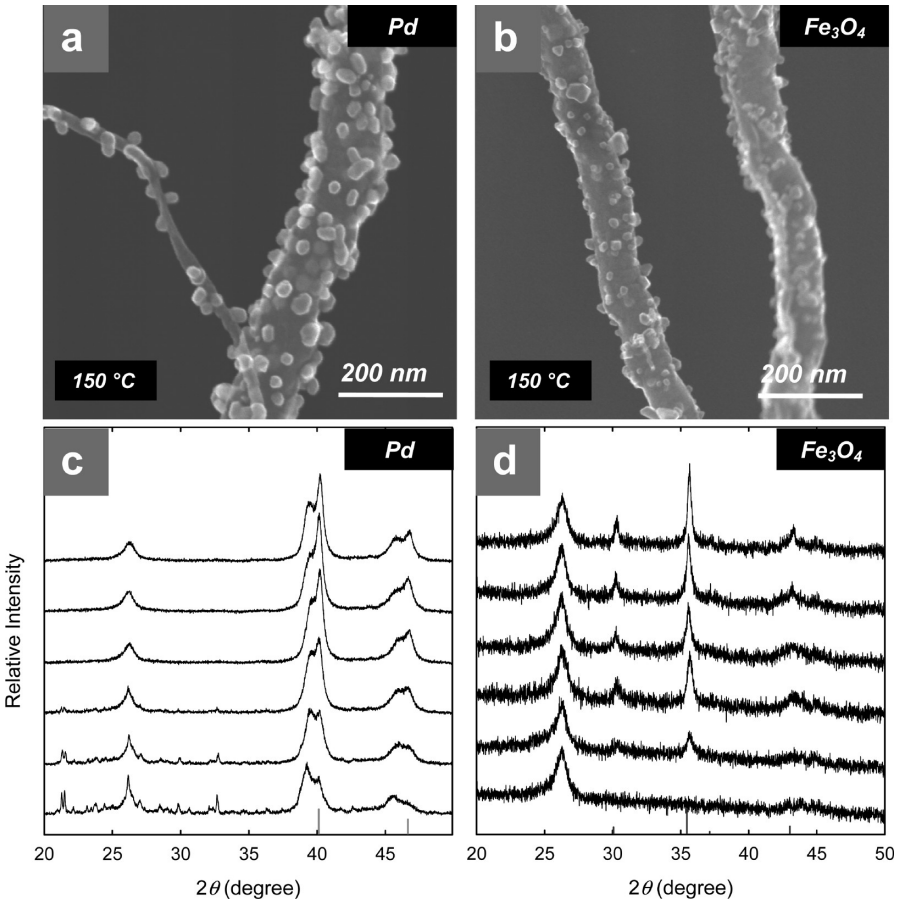

Figure 8. SEM images and the XRD patterns for (a,c) Pd vs (b,d) Fe_3O_4 nanoparticle-decorated MWCNTs from modulated microwave irradiation (maximum power =50 W) of mixtures of the nanotubes with the corresponding metal acetate salt (metal-to-C content were both 10 mol %) without further holding. (a,b) SEM images of samples heated to 150 °C. (c,d) XRD patterns of samples heated to (from bottom to top) 50, 100, 150, 200, 250, and 300 °C, respectively. The ICDD PDF patterns for Pd (#05−0681) and Fe_3O_4 (#01−1111) are also shown for comparison.

from both Pd (Figure 8c) and Fe_3O_4 (Figure 8d), corresponding to the increase of salt conversion into the respective nanoparticles. In the XRD patterns of Pd-decorated MWCNTs, similar doublet peaks were previously observed and attributed to partially enlarged unit cell from either a rather uniform strain from substrate attachment or inclusion of oxygen or carbon atoms for the peak positions with lower 2θ values.[25]

Whether an organic salt decomposes into its corresponding metal, metal oxide, or a mixture as well as the size ranges of the resultant nanoparticles is typically intrinsic to the salt composition, as was shown in our previous studies.[23] Importantly, the temperature ramping profiles of both palladium acetate/and iron acetate/MWCNT systems (not shown) were quite similar to the silver acetate/MWCNT system in spite of iron acetate decomposing into oxide nanoparticles with much lower microwave absorptivity compared to silver and palladium metals. This strongly suggested that the MWCNT substrates were the dominant microwave absorbers for salt decomposition in these reactions and the absorptivity of the metal or metal oxide particle that was formed had only a minor influence in the specified conditions.

Microwave vs Conventional Heating in Pt-MWCNT System. In the silver acetate/MWCNT model system, the rapid temperature ramping via microwave heating resulted in broader size distribution and slightly larger average particle size of Ag nanoparticles compared to conventional heating under a nitrogen atmosphere.[23] The increase in metal nanoparticle size using microwave heating was much more evident in the platinum acetylacetonate/MWCNT system. The modulated microwave heating of a 1 mol % Pt-to-C salt/nanotube mixture (~ 60 mg in each reaction) was carried out with 300 W maximum power at a set temperature of 300 °C (platinum acetylacetonate decomposition temperature ~265 °C). Under these conditions, the temperature ramping of the mixture took ~40 s (ramp rate ~450 °C/min). As shown in Figure 9a, the samples after temperature ramping with further hold times of 0, 2, and 10 min showed essentially the same XRD patterns with the expected Pt peaks (e.g., 39.9° (111) and 46.3° (200), ICDD #04−0802) of similar intensities as well as the (002) peak from MWCNTs at 26.2°. The sizes of Pt nanoparticles decorated on MWCNT surfaces were all within the range of 5 − 7 nm (Figure 9b−d). These results suggested that the decomposition of platinum acetylacetonate into Pt metal was completed within the temperature ramp time and further hold in the microwave reactor had negligible effect on the particle sizes and overall sample morphology, as was shown for the silver acetate/MWCNT system.

The samples prepared using conventional heating in a nitrogen oven with a much slower ramp rate (~5 °C/min) showed distinctively different XRD patterns (Figure 9e) and particle size distribution (Figures 9f−h). The XRD spectra from conventional

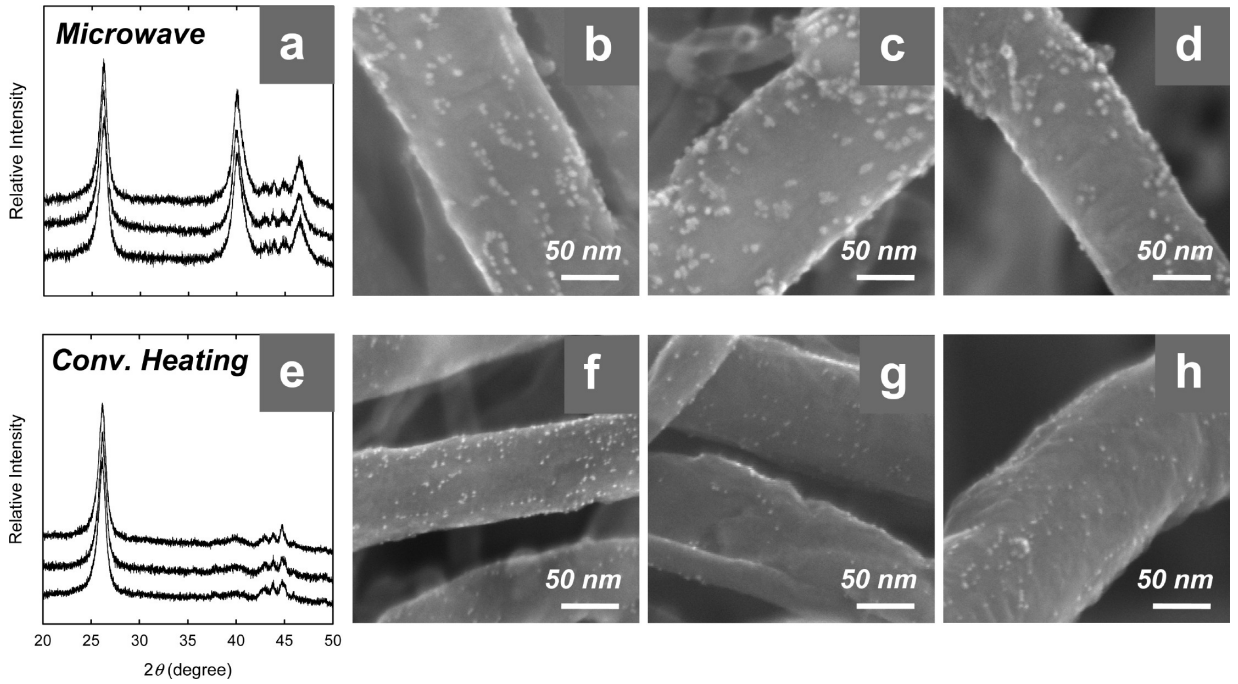

Figure 9. XRD patterns and SEM images of Pt nanoparticle-decorated MWCNTs from microwave heating vs conventional heating. The XRD patterns in (a) were from modulated microwave heating (maximum power = 300 W) of the same platinum acetylacetonate/MWCNT mixture (10 mol % Pt-to-C content) with hold times of (from bottom to top) 0, 1, and 5 min after ramping to the set temperature of 300 °C. SEM images of these samples are shown in b–d, respectively. (e) XRD patterns for comparison from conventional heating of the same salt–nanotube mixture to (from bottom to top) 300, 350, and 450 °C (ramp rate ~5.4 °C/min) with hold times of 3 h. SEM images of these samples are shown in f–h, respectively.

heating to 300, 350, and 450 °C with 3 h holds were similar to one another in that the Pt (111) peaks were all present but only marginally detectable. This is in contrast to the prominent peaks for identical samples prepared using microwave heating in Figure 9a. Presumably the difference in XRD peak intensity is due to the smaller size of the Pt nanoparticles from conventional heating being close to the threshold of XRD detection limit, thus yielding much broadened peak signals. SEM characterization (Figures 9f–h) confirmed that the nanoparticles from conventional heating were of 2–3 nm in size, significantly smaller than those prepared from microwave heating.

Other Carbon and Non-Carbon Substrates. Solid SWCNT powder was an effective substrate for solvent-free microwave heating as well, with temperature ramp rate and salt conversion profiles being very similar to those observed with MWCNT substrates (data not shown). Metal and metal oxide depositions onto other carbon and noncarbon substrates by microwave heating were also successfully demonstrated. Because it was shown herein that the use of different salts had little effect on the temperature ramping profiles during modulated microwave heating, it was of interest to investigate whether the different microwave absorption characteristics of the substrate materials would affect the reaction course and outcome. Thus, EG and h-BN powder substrates, both with high thermal conductivities but the latter having less microwave absorbing characteristics, were selected as substrates for comparison.

As shown in Figure 10, the ramp time of a silver acetate/EG mixture (~10 mol % Ag-to-C) with modulated microwave heating (maximum power = 50 W) was very similar to that of an identical sample with MWCNTs as the substrate (Figure 3). For example, it took 16 and 10 s for the mixtures to be heated to 150 °C, and 125 and 120 s to 300 °C, for the EG and MWCNT systems, respectively. In sharp contrast, the heating of a silver acetate/h-BN mixture (~20 mol % Ag-to-BN, comparable to ~10 mol % Ag-to-C in weight percentage) took 207 and 476 s to reach 150 and 300 °C, respectively, with a set maximum power of 300 W (the actual power level mostly stayed at 300 W). The use of electrically and thermally insulating silica–alumina particles ("lunar dust simulant" particles) as the alternative substrate for Ag nanoparticle growth also provided similarly slow ramping rates (141 and 494 s to 150 and 300 °C, respectively, at 300 W with ~30 wt % Ag). Because the thermal conductivities of h-BN and EG are of the same order of magnitude, the above results strongly suggested that it was the microwave absorption capability of the substrate, rather than its thermal conductivity, that had the most impact on the temperature ramp rates. The salt-to-metal conversions of these poor microwave-absorbing substrates were only complete at high set temperatures (300 °C for h-BN). Nevertheless, metallic Ag nanoparticles were also formed as a result and were comparable in size to those prepared using EG as the substrate (see Figure S2 in the Supporting Information).

It is interesting to point out the difference between using microwave energy and mechanical energy via ball-milling, where thermal conductivity of the substrate was a dominant factor in the heating.[24] In those reactions, the use of h-BN and EG as substrates provided similar results in effective salt decomposition, while the use of thermally insulating substrates (i.e., silica–alumina microspheres) showed poor salt-to-metal conversion.

Graphene as Substrate. Graphene materials have attracted extraordinary attention recently because their excellent electronic, mechanical, and thermal properties may out-perform CNTs in many applications but at lower cost.[79,80] Solid graphene powder (mostly from processes involving reduction of graphene oxide) has already become commercially available from various

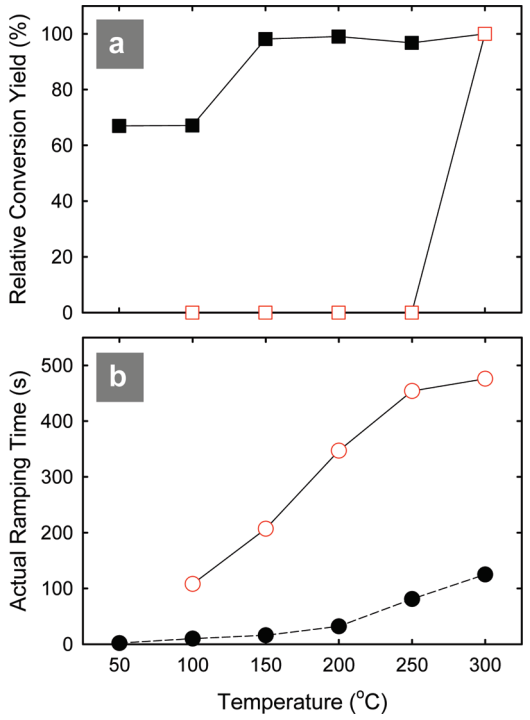

Figure 10. (a) Relative conversion yields and (b) ramp times of samples from modulated microwave heating of mixtures of silver acetate with EG (solid black symbols, maximum power = 50 W) and h-BN (open red symbols, maximum power = 300 W) at Ag-to-substrate contents of 10 and 20 mol %, respectively, to various temperatures without further holding. The relative conversion yields were calculated by $(\text{yield}\%)_T = [(I_{Ag}/I_{(002)})_T/(I_{Ag}/I_{(002)})_{300\ °C}] \times 100\%$, where $I_{(002)}$ corresponds to the (002) peak of EG or h-BN and T corresponds to the set temperature.

vendors in large quantities and is ideal for the use as substrate to support metal and metal oxide nanoparticles using our solvent-free heating techniques. Mixtures of graphene with various salts (metal-to-C contents ~10 mol % except for Pt and Au, which were at ~5 mol %) were heated using "no hold" modulated microwave irradiation (maximum power = 50 W). The set temperature was 300 °C and the ramp time for all experiments took 70 − 100 s regardless of the salts used. This observation is consistent with those in previous sections using other carbon substrates, indicating the dominant role of graphene in the microwave absorption during irradiation. As shown in the TEM images in Figure 11, the products contained few-layered graphene structures with surfaces decorated with nanoparticles of various average sizes. The corresponding XRD patterns (Figure 11 insets, C(002) peak at ~26° for graphene is weak/broad for all samples) confirmed that these nanoparticles were in the forms of metal (Ag, Pd, Pt, Au, Ni; red standard patterns), metal oxide (Fe_3O_4, TiO_2, and MnO; blue standard patterns), or their mixture (Co/CoO). The crystallinity of these nanoparticles was further confirmed by using HR-TEM and SAED (see Figures S3 and S4 in the Supporting Information). Again, the characteristics of the starting salt intrinsically determined the relative size range (e.g., sub-5 nm Pt and TiO_2 nanoparticles vs 5−15 nm Pd and Fe_3O_4 nanoparticles at ~5−10 mol % loading; also see Figure S5 in the Supporting Information), morphology (e.g., single-crystal Pt nanoparticles vs globular Co/CoO clusters), and chemical composition (metal vs metal oxide) of the graphene-attached metal or metal oxide nanoparticles. It is also noted that the nanoparticles formed on graphene surfaces were usually smaller than those on other carbon substrates, likely due to the much lower density (~10 g/L) and higher available surface area of the graphene powder compared to nanotubes (density ~200 g/L for MWCNTs) in the current study.

Carbon Nanotube Yarn as Substrate. Although the substrates used in all experiments shown so far were solid powder materials, the present method to generate metal or metal oxide nanoparticles by using microwave (or conventional) heating is very versatile with respect to the form of substrate used. For example, carbon nanotube yarns (mainly consisting of large-diameter SWCNTs) can be used as the substrate material for the decoration of different metal or metal oxide nanoparticles. Because solid-state mixing is no longer practical in this case, the yarns were soaked in a salt solution (e.g., 0.05 M palladium acetate in ethanol or titanium acetylacetonate in acetone) for ~15 min followed by solvent evaporation. As shown in Figure 12, very brief continuous microwave irradiation (50 W, 10 s) of the salt-infused yarns in the microwave reactor resulted in rapid nanoparticle (Pd and TiO_2) formation on the nanotube surfaces. The respective nanoparticle sizes are comparable to those observed for all-solid-state reactions described above. It could thus be envisioned that large scale decoration of similar yarn or fiber materials with metal or metal oxide nanoparticles could be achieved with a rapid, continuous process in which the yarn is first passed through a salt solution followed by a short microwave heating zone.

Surface-Enhanced Raman Spectroscopy (SERS). Although discovered decades ago, SERS has recently attracted significant attention for ultrasensitive trace detections due to the success in the synthetic approaches for active nanoscale metal substrates of various compositions and configurations.[81,82] While regular Raman scattering is a relatively weak process, signals of analytes absorbed on specific metal (e.g., Ag and Au) surfaces can be significantly enhanced because of the localized surface plasmon resonance of the metal. Although neat metal nanoparticles have been widely used, nanocarbon materials such as CNTs and graphene have been suggested to support these nanoparticles for SERS.[83−86] The use of nanocarbon supports comes with benefits such as the prevention of nanoparticle aggregation (especially in solid state) and sometimes the quenching of fluorescence interference of the analytes, thus preserving or even enhancing the SERS properties of the nanoparticles. It was also suggested that the surface roughness of a SERS-active metal substrate (or, comparably, the size of metal nanoparticles) of 10−100 nm scale is often ideal for signal enhancement. For the present method in this report, the diameters of Ag nanoparticles decorated on MWCNTs obtained from microwave irradiation are in this range, making them suitable candidates for potential SERS applications. The Raman signal enhancement of MWCNTs by the attached Ag nanoparticles was already discussed in an earlier section.

Rhodamine 6G (R6G) was used as the model analyte for SERS studies using the Ag-MWCNT samples as the substrate. In each experiment, a 10 μL drop of a R6G ethanol solution was applied to a given powder sample. After evaporating the solvent, several Raman spectra were obtained from different locations of the sample and averaged. R6G has multiple peaks in the region of 600−1700 cm^{-1}. As shown in Figure 13a, while no R6G signals could be detected at a concentration of 10^{-5} M when pristine MWCNTs were used as substrate, the fingerprint peaks became much more enhanced with Ag-MWCNT substrates. The

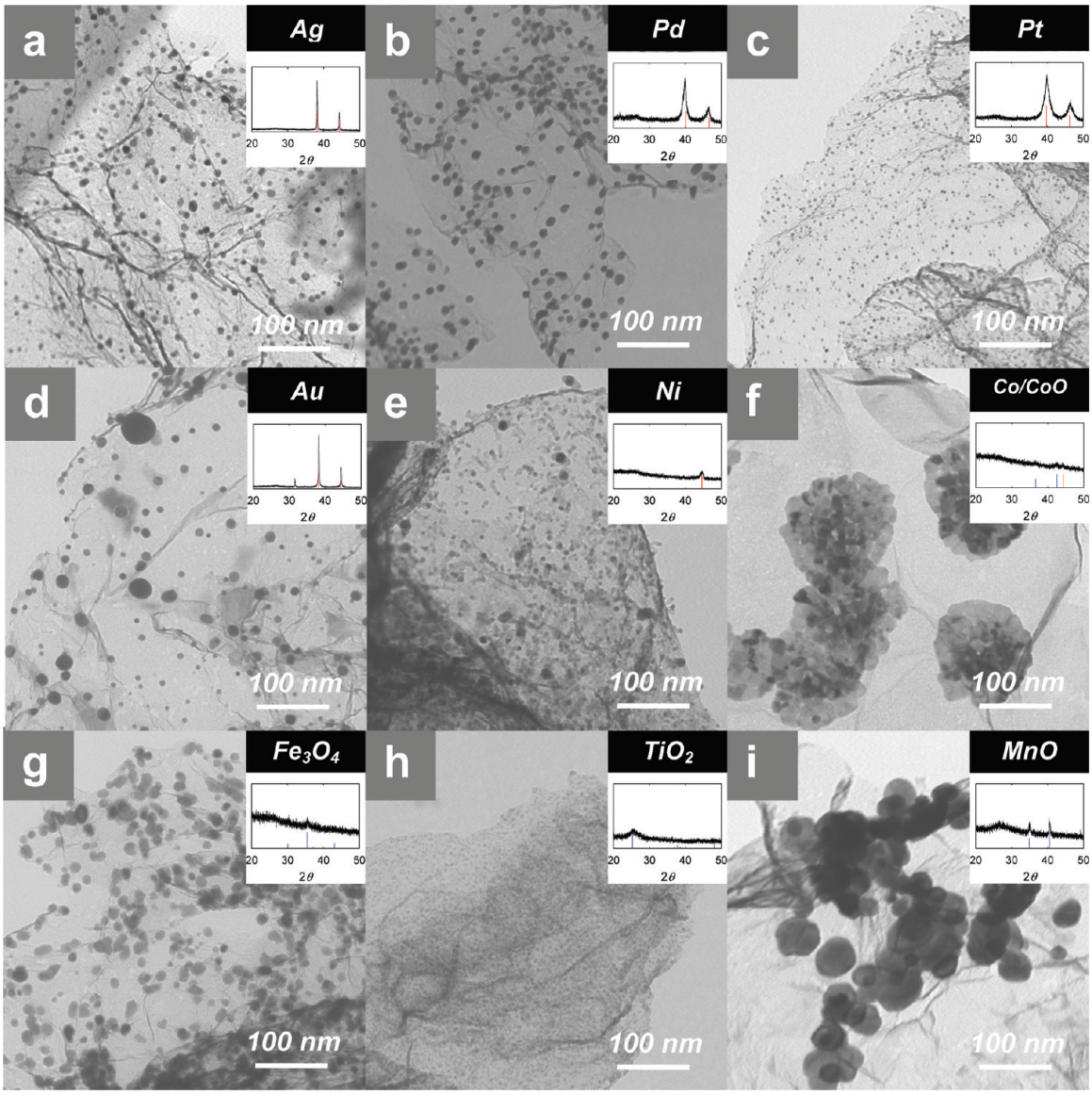

Figure 11. TEM images of various metal or metal oxide nanoparticle-decorated graphene samples from modulated microwave heating (maximum power = 50 W, set temperature = 300 °C) of the corresponding salt/graphene solid mixtures. XRD patterns in the insets confirmed the identities of the nanoparticles in the images being (a) Ag (ICDD #04−0783), (b) Pd (#05−0681), (c) Pt (#04−0802), (d) Au (#04−0784), (e) Ni (#01−1260), (f) Co/CoO (#01−1255/#01−1227), (g) Fe_3O_4 (#01−1111), (h) TiO_2 (#21−1272), and (i) MnO (#07−0230), respectively. The metal-to-C contents in all samples were ∼10 mol % except for c and d, which were both ∼5 mol %.

sample with higher Ag loading provided with more significant enhancement, likely associated with the larger nanoparticle size and closer particle−particle distance in the sample. Although the higher wavenumber peaks of R6G overlapped with the D- and G-bands of MWCNTs, the two peaks at 609 and 771 cm^{-1} can be clearly identified with no interference.

The SERS effect of CNT yarns decorated with Ag nanoparticles was also tested in a set of proof-of-concept experiments. Similar to those described in the last section, the specimen was prepared by soaking the yarn sample in a 0.005 M aqueous silver acetate solution for 15 min followed by brief microwave irradiation of 15 s at 50 W. As a result, Ag nanoparticles with sizes in the range of 5−50 nm were formed on the surfaces of CNTs in the yarn (see Figure S6 in the Supporting Information). R6G ethanol solutions (10 μL each) were similarly applied to the Ag-decorated CNT yarn sample followed by solvent evaporation. The signals of R6G were also much enhanced (Figure 13b) despite somewhat lower efficiency in comparison with the use of the Ag-MWCNT powder samples at the same analyte concentration. This is somewhat expected since the yarn has relatively smaller surface area than the nanotube powder in general, thus rendering less SERS-active hot spots per unit area. Other possible causes may include the difference in particle size and interparticle distance and ingression of the metal nanoparticles into the interstices of the yarn. It should be realized that this procedure to prepare the Ag-CNT yarn is still far from optimized, but nevertheless showed great potential in the construction of durable SERS sensors.

Conclusions and Outlook. Microwave irradiation was shown to be an effective energy source for the rapid decomposition of organic metal salts in a solid mixture with various nanoscale substrates

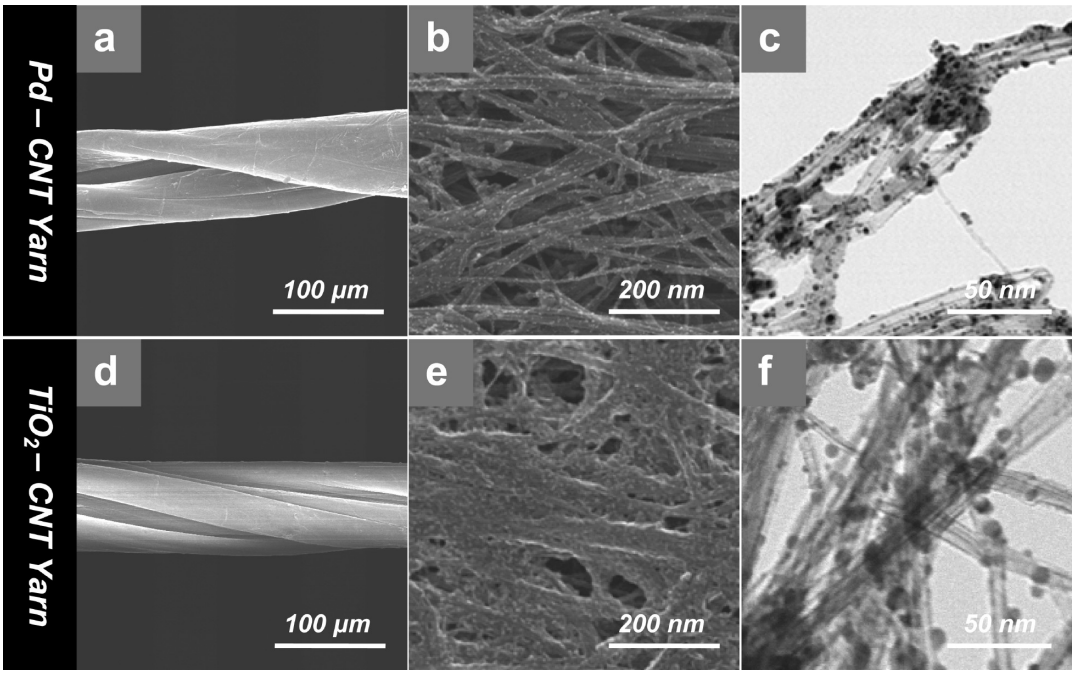

Figure 12. SEM images at (a,d) lower and (b,e) higher magnifications and (c, f) TEM images of carbon nanotube yarns decorated with (a−c) Pd and (d−f) TiO_2 nanoparticles from 10 s of continuous microwave irradiation at 50 W of the corresponding salt-soaked CNT yarns.

under completely solvent-free conditions. An important advantage of the method is that no further product purification is needed except for brief drying because all reaction byproducts are volatile. The results showed that substrates with good microwave absorptivity such as carbon (e.g., MWCNTs, SWCNTs, EG, and graphene) underwent rapid Joule heating along the substrate body. The local heating of the carbon substrates decomposed the nearby salt particles to afford the near instantaneous formation of metal or metal oxide nanoparticles, decorating the substrate surfaces within seconds of microwave exposure. The complete salt-to-metal conversion for the silver acetate/MWCNT system, for example, could be completed in a matter of seconds under certain conditions. It was shown that the nanoparticle sizes from modulated microwave irradiation were similar to those from conventional heating and could be tuned by the metal content in the sample, with little dependence on the set temperature and further residence time at that temperature. Raman studies showed that the MWCNT structures were little affected even with prolonged modulated microwave irradiation. In the silver acetate/MWCNT system, it was found that the high rate of microwave heating could result in the formation of small nanoparticles along with much larger ones (likely the consequence of incomplete thermodynamic Ag nanoparticle growth); this was more obvious for samples with higher salt loading and especially those from continuous microwave irradiation ("Power-Time Mode").

The present method was shown to be widely applicable to various organic metal salts and different carbon and noncarbon substrates. Each precursor salt has a particular thermal decomposition process with consistent metal or metal oxide products. However, reaction profiles (ramp times and conversion yields) were not significantly affected by the salt used (and thus the nanoparticles produced), but were directly related to the microwave absorptivity of the substrate. The latter was unambiguously demonstrated by the drastic differences in the temperature ramp times and salt conversions between good (e.g., EG) and poor

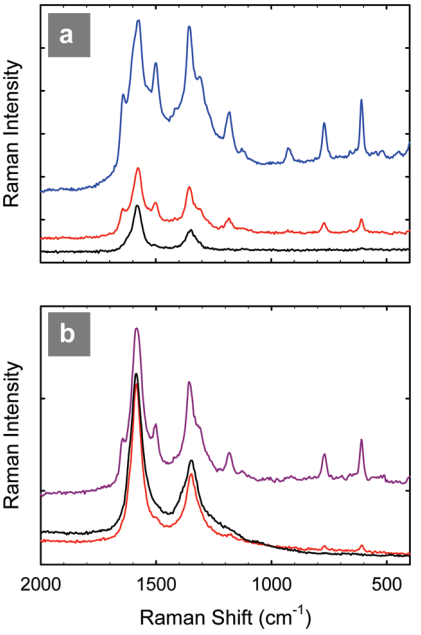

Figure 13. Raman spectra from SERS studies (532 nm excitation) of R6G on CNT and Ag-CNT substrates: (a) R6G (from a 1×10^{-5} M ethanol solution) on pristine MWCNTs (black) and Ag-MWCNT samples with 1 mol % (red) and 10 mol % (blue) Ag-to-C contents; (b) a CNT yarn sample decorated with Ag nanoparticles (black) and the same yarn applied with 1×10^{-5} M (red) and 1×10^{-4} M (purple) R6G ethanol solutions.

(e.g., h-BN) microwave absorbing substrates. In contrast to previous studies using conventional heating under nitrogen atmosphere (substrate independent) or mechanical energy (preferably with thermally conductive substrates), high microwave absorptivity of the substrate is an important consideration

when using microwave heating for nanoparticle decoration. The versatility of the method was further demonstrated with the use of graphene as substrate for the decoration with a variety of metal or metal oxide nanoparticles, and also h-BN and lunar dust simulant as substrates. The latter two insulating materials required longer microwave exposure times, but resulted in nanoparticle size distributions comparable to carbon substrates. Despite the fast reaction rates, most of the metal and metal oxide nanoparticles were formed by templating on the respective substrate as seen from the flat interface between these nanoparticles and said substrate, similar to the mechanism with conventional heating.[23]

The solvent-free microwave heating method is a much more rapid and thus higher throughput alternative to the effective and scalable conventional heating method previously reported.[23] The successful use of substrate materials of nonpowder forms such as carbon nanotube yarns and the rapid nature of the process not only demonstrated the versatility of the method, but also strongly suggested that this process may be amenable to scale-up for industrial production of metal or metal oxide nanoparticle-decorated materials with different compositions or morphologies.

The potential SERS applications of Ag nanoparticle decorated-MWCNTs and CNT yarns were demonstrated. However, it is only one of many potential uses of such nanohybrid materials and the synthetic methodology itself. Because of the high throughput nature, it is highly anticipated that the method (with either microwave or conventional heating) would become useful because it enables rapid preparation of metal−carbon nanohybrids materials that can be subsequently screened for various electrical, composite, energy, catalysis, and biological applications.

■ ASSOCIATED CONTENT

Supporting Information. Raman spectra of Ag-MWCNT samples from modulated microwave heating of different hold times, SEM images of Ag-EG and Ag-BN samples, HR-TEM and size-distribution plots of the various metal and metal oxide nanoparticles decorated on graphene, SAED spectra of Pd-graphene and Pt-graphene samples, and SEM images of Ag nanoparticle-decorated CNT yarns. This material is available free of charge via the Internet at http://pubs.acs.org.

■ AUTHOR INFORMATION

Corresponding Author

*E-mail: yi.lin-1@nasa.gov (Y.L.); john.w.connell@nasa.gov (J.W.C.).

■ ACKNOWLEDGMENT

D.W.B. is an undergraduate student at Virginia Commonwealth University and was an awardee of the Langley Aerospace Research Summer Scholars (LARSS) Program. The authors thank D. Hartman (Lockheed Martin/NASA Langley Research Center) for XRD measurements. We are grateful to Prof. H. Elsayed-Ali and Dr. W. Cao (Applied Research Center, Old Dominion University) for their help in the HR-TEM and SAED analyses.

■ REFERENCES

(1) Wildgoose, G. G.; Banks, C. E.; Compton, R. G. *Small* **2006**, *2*, 182.
(2) Georgakilas, V.; Gournis, D.; Tzitzios, V.; Pasquato, L.; Guldi, D.; Prato, M. *J. Mater. Chem.* **2007**, *17*, 2679.
(3) Kamat, P. V. *J. Phys. Chem. Lett.* **2010**, *1*, 520–527.
(4) Corma, A.; Garcia, H.; Leyva, A. *J. Mol. Catal. A: Chem.* **2005**, *230*, 97–105.
(5) Karousis, N.; Tsotsou, G. E.; Evangelista, F.; Rudolf, P.; Ragoussis, N.; Tagmatarchis, N. *J. Phys. Chem. C* **2008**, *112*, 13463–13469.
(6) Scheuermann, G. M.; Rumi, L.; Steurer, P.; Bannwarth, W.; Mulhaupt, R. *J. Am. Chem. Soc.* **2009**, *131*, 8262–8270.
(7) Li, Y.; Fan, X.; Qi, J.; Ji, J.; Wang, S.; Zhang, G.; Zhang, F. *Nano Res.* **2010**, *3*, 429–437.
(8) Kamat, P. V. *J. Phys. Chem. C* **2007**, *111*, 2834–2860.
(9) Moriguchi, I.; Hidaka, R.; Yamada, H.; Kudo, T.; Murakami, H.; Nakashima, N. *Adv. Mater.* **2006**, *18*, 69–73.
(10) Wang, D.; Choi, D.; Li, J.; Yang, Z; Nie, Z.; Kou, R.; Hu, D.; Wang, C.; Saraf, L. V.; Zhang, J.; Aksay, I.; Liu, J. *ACS Nano* **2009**, *3*, 907–914.
(11) Zhang, H.; Cao, G.; Wang, Z.; Yang, Y.; Shi, Z.; Gu, Z. *Nano Lett.* **2008**, *8*, 2664–2668.
(12) Yan, J.; Fan, Z.; Wei, T.; Cheng, J.; Shao, B.; Wang, K.; Song, L.; Zhang, M. *J. Power Sources* **2009**, *194*, 1202–1207.
(13) Chen, S.; Zhu, J.; Wu, X.; Han, Q.; Wang, X. *ACS Nano* **2010**, *4*, 2822–2830.
(14) Hou, Y.; Cheng, Y.; Hobson, T.; Liu, J. *Nano Lett.* **2010**, *10*, 2727–2733.
(15) Wang, H.; Cui, L.-F.; Yang, Y.; Casalongue, H. S.; Robinson, J. T.; Liang, Y.; Cui, Y.; Dai, H. *J. Am. Chem. Soc.* **2010**, *132*, 13978–13980.
(16) Han, W.-Q.; Zettl, A. *Nano Lett.* **2003**, *3*, 681–683.
(17) Wen, Z.; Wang, Q.; Zhang, Q.; Li, J. *Adv. Func. Mater.* **2007**, *17*, 2772–2778.
(18) Wang, D.; Kou, R.; Choi, D.; Yang, Z.; Nie, Z.; Li, J.; Saraf, L.; Hu, D.; Zhang, J.; Graff, G.; Liu, J.; Pope, M. A.; Aksay, I. A. *ACS Nano* **2010**, *4*, 1587–1595.
(19) Ban, C.; Wu, Z.; Gillaspie, D. T.; Chen, L.; Yan, Y.; Blackburn, J. L.; Dillon, A. C. *Adv. Mater.* **2010**, *22*, E145–E149.
(20) Zhang, M.; Lei, D.; Yin, X.; Chen, L.; Li, Q.; Wang, Y.; Wang, T. *J. Mater. Chem.* **2010**, *20*, 5538–5543.
(21) He, H.; Gao, C. *ACS Appl. Mater. Interfaces* **2010**, *2*, 3201–3210.
(22) Planeix, J. M.; Coustel, N.; Coq, J.; Brotons, V.; Kumbhar, P. S.; Dutartre, R.; Geneste, P.; Bernier, P.; Ajayan, P. M. *J. Am. Chem. Soc.* **1994**, *116*, 7935–7936.
(23) Lin, Y.; Watson, K. A.; Fallbach, M. J.; Ghose, S.; Smith, J. G.; Delozier, D. M.; Cao, W.; Crooks, R. E.; Connell, J. W. *ACS Nano* **2009**, *3*, 871.
(24) Watson, K. A.; Fallbach, M. J.; Ghose, S.; Smith, J. G.; Delozier, D. M.; Connell, J. W. . U.S. Patent 7 704 553, April 27, 2010.
(25) Lineberry, Q. J.; Cao, Y.; Lin, Y.; Ghose, S.; Connell, J. W.; Pan, W.-P. *Energy Fuels* **2009**, *23*, 1512.
(26) Lin, Y.; Watson, K. A.; Ghose, S.; Smith, J. G.; Williams, T. V.; Crooks, R. E.; Cao, W.; Connell, J. W. *J. Phys. Chem. C* **2009**, *113*, 14858–14862.
(27) Caddick, S. *Tetrahedron* **1995**, *51*, 10403–10432.
(28) Kappe, C. O. *Chem. Soc. Rev.* **2008**, *37*, 1127–1139.
(29) Polshettiwar, V.; Nadagouda, M. N.; Varma, R. S. *Aust. J. Chem.* **2009**, *62*, 16–26.
(30) Bilecka, I.; Niederberger, M. *Nanoscale* **2010**, *2*, 1358–1374.
(31) Vazquez, E.; Prato, M. *ACS Nano* **2010**, *3*, 3819–3824.
(32) Wadhawam, A.; Garrett, D.; Perez, J. M. *Appl. Phys. Lett.* **2003**, *83*, 2683–2685.
(33) Imholt, T. J.; Dyke, C. A.; Hasslacher, B.; Perez, J. M.; Price, D. W.; Roberts, J. A.; Scott, J. B.; Wadhawan, A.; Ye, Z.; Tour, J. M. *Chem. Mater.* **2003**, *15*, 3969–3970.
(34) Paton, K. R.; Windle, A. H. *Carbon* **2008**, *46*, 1935–1941.
(35) Ye, Z.; Deering, W. D.; Krokhin, A.; Roberts, J. A. *Phys. Rev. B* **2006**, *74*, 075425.
(36) Liu, Z.; Bai, G.; Huang, Y.; Li, F.; Ma, Y.; Guo, T.; He, X.; Lin, X.; Gao, H.; Chen, Y. *J. Phys. Chem. C* **2007**, *111*, 13696–13700.
(37) Alvarez-Zauco, E.; Basiuk, V. A.; Acosta-Najarro, D.; Flores-Morales, C.; Puente-Lee, I.; Bassiouk, M.; Gromovoy, T. Y.; Mischanchuk, B. G.; Basiuk, E. V. *J. Nanosci. Nanotechnol.* **2010**, *10*, 448–455.

(38) Lin, W.; Moon, K.-S.; Zhang, S.; Ding, Y.; Shang, J.; Chen, M.; Wong, C.-P. *ACS Nano* **2010**, *4*, 1716.
(39) Tasis, D.; Tagmatarchis, N.; Bianco, A.; Prato, M. *Chem. Rev.* **2006**, *106*, 1105–1136.
(40) Della Negra, F.; Meneghetti, M.; Menna, E. *Fullerenes, Nanotubes, Carbon Nanostruct.* **2003**, *11*, 25–34.
(41) Wang, Y.; Iqbal, Z.; Mitra, S. *Carbon* **2005**, *43*, 1015–1020.
(42) Delgado, J. L.; De la Cruz, P.; Langa, F.; Urbina, A.; Casado, J.; Lopez; Navarrete, J. T. *Chem. Commun.* **2004**, 1734–1735.
(43) Li, J.; Grennberg, H. *Chem.—Eur. J.* **2006**, *12*, 3869–3875.
(44) Liu, J.; Zubiri, M. R. I.; Vigolo, B.; Dossot, M.; Fort, Y.; Ehrhardt, J. J.; McRae, E. *Carbon* **2007**, *45*, 885–891.
(45) Umeyama, T.; Tezuka, N.; Fujita, M.; Matano, Y.; Takeda, N.; Murakoshi, K.; Yoshida, K.; Isoda, S.; Imahori, H. *J. Phys. Chem. C* **2007**, *111*, 9734–9741.
(46) Xu, Y.; Wang, X.; Tian, R.; Li, S.; Wan, L.; Li, M.; You, H.; Li, Q.; Wang, S. *Appl. Surf. Sci.* **2008**, *254*, 2431–2435.
(47) Guryanov, I.; Toma, F. M.; Lopez, A. M.; Carraro, M.; Ros, T. D.; Angelini, G.; D'Aurizio, E.; Fontana, A.; Maggini, M.; Prato, M. *Chem.—Eur. J.* **2009**, *15*, 12837–12845.
(48) Colomer, J.-F.; Marega, R.; Traboulsi, H.; Meneghetti, M.; Tendeloo, G. V.; Bonifazi, D. *Chem. Mater.* **2009**, *21*, 4747–4749.
(49) Brunetti, F. G.; Herrero, M. A.; de M. Munoz, J.; Glordanl, S.; Diaz-Ortiz, A.; Filippone, S.; Ruaro, G.; Meneghetti, M.; Prato, M.; Vazquez, E. *J. Am. Chem. Soc.* **2007**, *129*, 14580–14581.
(50) Brunetti, F. G.; Herrero, M. A.; de M. Munoz, J.; Diaz-Ortiz, A.; Alfonsi, J.; Meneghetti, M.; Prato, M.; Vazquez, E. *J. Am. Chem. Soc.* **2008**, *130*, 8094–8100.
(51) Higginbotham, A. L.; Moloney, P. G.; Waid, M. C.; Duque, J. G.; Kittrell, C.; Schmidt, H. K.; Stephenson, J. J.; Arepalli, S.; Yowell, L. L.; Tour, J. M. *Compos. Sci. Technol.* **2008**, *68*, 3087–3092.
(52) Wang, C.; Chen, T.; Chang, S.; Cheng, S.; Chin, T. *Adv. Func. Mater.* **2007**, *17*, 1979–1983.
(53) Chen, W.; Yan, L.; Bangal, P. R. *Carbon* **2010**, *48*, 1146–1152.
(54) Zhu, Y.; Murali, S.; Stoller, M. D.; Velamakanni, A.; Piner, R. D.; Ruoff, R. S. *Carbon* **2010**, *48*, 2118–2122.
(55) Murugan, A. V.; Muraliganth, T.; Manthiram, A. *Chem. Mater.* **2009**, *21*, 5004–5006.
(56) Li, Z.; Yao, Y.; Lin, Z.; Moon, K.-S.; Lin, W.; Wong, C. *J. Mater. Chem.* **2010**, *20*, 4781–4783.
(57) Melucci, M.; Treossi, E.; Ortolani, L.; Giambastiani, G.; Morandi, V.; Klar, P.; Casiraghi, C.; Samori, P.; Palermo, V. *J. Mater. Chem.* **2010**, *20*, 9052–9060.
(58) Bai, J. Y.; Xu, Z. D.; Zheng, Y. F. *Chem. Lett.* **2006**, *35*, 96–97.
(59) Raghuveer, M. S.; Agrawal, S.; Bishop, N.; Ramanath, G. *Chem. Mater.* **2006**, *18*, 1390–1393.
(60) Kim, S. J.; Park, Y. J.; Ra, E. J.; Kim, K. K.; An, K. H.; Lee, Y. H.; Choi, J. Y.; Park, C. H.; Doo, S. K.; Park, M. H.; Yang, C. W. *Appl. Phys. Lett.* **2007**, *90*, 023114.
(61) Duque, J. G.; Pasquali, M.; Schmidt, H. K. *J. Am. Chem. Soc.* **2008**, *130*, 15340–15347.
(62) Poh, C. K.; Lim, S. H.; Pan, H.; Lin, J.; Lee, J. Y. *J. Power Sources* **2008**, *176*, 70–75.
(63) Wang, S.; Wang, X.; Jiang, S. P. *Langmuir* **2008**, *24*, 10505–10512.
(64) Wang, S.; Jiang, S. P.; White, T. J.; Guo, J.; Wang, X. *J. Phys. Chem. C* **2009**, *113*, 18935–18945.
(65) Zhang, W.; Chen, J.; Swiegers, G. F.; Ma, Z.-F.; Wallace, G. G. *Nanoscale* **2010**, *2*, 282–286.
(66) Dennany, L.; Sherrell, P.; Chen, J.; Innis, P. C.; Wallace, G. G.; Minett, A. I. *Phys. Chem. Chem. Phys.* **2010**, *12*, 4135–4141.
(67) Sherrell, P. C.; Chen, J.; Razal, J. M.; Nevirkovets, I. P.; Crean, C.; Wallace, G. G.; Minett, A. I. *Energy Environ. Sci.* **2010**, *3*, 1979–1984.
(68) Hasson, H. M. A.; Abdelsayed, V.; Khder, A. E. R. S.; AbouZeid, K. M.; Terner, J.; El-Shall, M. S.; Al-Resayes, S. I.; El-Azhary, A. A. *J. Mater. Chem.* **2009**, *19*, 3832–3837.
(69) Jasuja, K.; Linn, J.; Melton, S.; Berry, V. *J. Phys. Chem. Lett.* **2010**, *1*, 1853–1860.
(70) Guo, S.; Wen, D.; Zhai, Y.; Dong, S.; Wang, E. *ACS Nano* **2010**, *4*, 3959–3968.
(71) Yan, J.; Wei, T.; Qiao, W.; Shao, B.; Zhao, Q.; Zhang, L.; Fan, Z. *Electrochim. Acta* **2010**, *55*, 6973–6978.
(72) Sharma, S.; Ganguly, A.; Papakonstantinou, P.; Miao, X.; Li, M.; Hutchison, J. L.; Delichatsios, M.; Ukleja, S. *J. Phys. Chem. C* **2010**, *114*, 19459–19466.
(73) The pressure level was not varied and left at the default value (0) in the programs. The actual pressure readings in most of these solid-state reactions built up to the range of 20−40 psi, which was apparently due to the gaseous salt decomposition products often including water vapor, CO_2, CO, and acetic acid.
(74) Lefrant, S.; Baltog, I.; de la Chapelle, M. L.; Baibarac, M.; Louarn, G.; Journet, C.; Bernier, P. *Synth. Met.* **1999**, *100*, 13–27.
(75) Corio, P.; Brown, S. D. M.; Marucci, A.; Pimenta, M. A.; Kneipp, K.; Dresselhaus, G.; Dresselhaus, M. S. *Phys. Rev. B* **2000**, *61*, 13202–13211.
(76) Chen, Y.-C.; Young, R. J.; Macpherson, J. V.; Wilson, N. R. *J. Phys. Chem. C* **2007**, *111*, 16167–16173.
(77) Chu, H.; Wang, J.; Ding, L.; Yuan, D.; Zhang, Y.; Liu, J.; Li, Y. *J. Am. Chem. Soc.* **2009**, *131*, 14310–14316.
(78) The microwave program automatically adjusted its power for the runs that took longer to ramp (e.g., targeting temperature >200 °C, ramp time >30 s). This means that the actual ramp time at those set conditions should have been much faster if the microwave power were kept constant.
(79) Geim, A. K. *Science* **2009**, *324*, 1530–1534.
(80) Zhu, Y.; Murali, S.; Cai, W.; Li, X.; Suk, J. W.; Potts, J. R.; Ruoff, R. S. *Adv. Mater.* **2010**, *22*, 3906–3924.
(81) Kneipp, K.; Kneipp, H.; Itzkan, I.; Dasari, R. R.; Feld, M. *Chem. Rev.* **1999**, *99*, 2957–2975.
(82) Doering, W. E.; Piotti, M. E.; Natan, M. J.; Freeman, R. G. *Adv. Mater.* **2007**, *19*, 3100–3108.
(83) Sanles-Sobrido, M.; Rodriguez-Lorenzo, L.; Lorenzo-Abalde, S.; Gonzalez-Fernandez, A.; Correa-Duarte, M. A.; Alvarez-Puebla, R. A.; Liz-Marzan, L. M. *Nanoscale* **2009**, *1*, 153–158.
(84) Sun, Y.; Liu, K.; Miao, J.; Wang, Z.; Tian, B.; Zhang, L.; Li, Q.; Fan, S.; Jiang, K. *Nano Lett.* **2010**, *10*, 1747–1753.
(85) Aldeanueva-Potel, P.; Correa-Duarte, M. A.; Alvarez-Puebla, R. A.; Liz-Marzan, L. M. *ACS Appl. Mater. Interfaces* **2010**, *2*, 19–22.
(86) Gonclaves, G.; Marques, P. A. A. P.; Granadeiro, C. M.; Nogueira, H. I. S.; Singh, M. K.; Gracio, J. *Chem. Mater.* **2009**, *21*, 4796–4802.